ChemComm

Dynamic Article Links ►

Cite this: DOI: 10.1039/c0xx00000x

www.rsc.org/xxxxxx

COMMUNICATION

# DNAzyme Tunable Lead (II) Gating Based on Ion-Track Etched Conical Nanochannels

**YanLi Shang,[a] Yuqi Zhang,[c] Pei Li,[c] Jing Lai,[a] Xiang-Yu Kong,[b] Weida Liu,[a] Kai Xiao,[d] Ganhua Xie,[d] Ye Tian,[d] Liping Wen[bd]* and Lei Jiang[bd]**

***Received (in XXX, XXX) Xth XXXXXXXXX 201X, Accepted Xth XXXXXXXXX 201X***
***First published on the web Xth XXXXXXXXX 201X***
**DOI: 10.1039/b000000x**

**A simple biomimetic ionic gate has been developed by modifying lead (Ⅱ) ions responsive DNAzymes onto the inner surface of ion-etched polymer nanochannels.**

Transportation between cells in multicellular organisms are performed usually by the sophisticated "gate mechanisms". For example, certain of ions passing the cell membranes are determined by the membrane bound proteins.[1] However, the biological membranes are not stable in changing external environments and artificial solid-state nanochannels are synthesized to mimic the membrane functions. Presently, synthetic special bio-mimetic materials, possessing similar function with biological materials in human life and industrial production, have been developed extensively due to their great flexibility based on geometry and size, excellent mechanical robustness, and multi-functional surface properties; especially the controllable nano-porous membranes are becoming a research hot topic in the biomimetic field.[2] So far, a lot of smart nanochannels have been developed. Siwy et al. reported a calcium induced voltage gating phenomenon in synthetic single conical nanopore.[3] Zheng et al. demonstrated a single biomimetic nanochannel that mimicking the binding and unbinding of ferrum (III) with transferrin.[4] Recently, our group have reported a series of researches about ion activated nanochannel, such as potassium ions,[2c] zinc ions,[2d] mercury ions[2g] and silver ions.[2h] Such biomimetic smart nanochannels have the potential to be used in mimicking switches in advanced devices.

Lead is highly toxic to many organs and tissues of human bodies including heart, bones, intestines, kidneys, reproductive and nervous systems. Especially, children are vulnerable to lead poisoning, which can severely affect mental and physical development; therefore, much effort is needed to deal with the lead eliminating. At present, EDTA (ethylene diamine tetraacetic acid) metal chelate and DMSA (dimercaptosuccinic acid) competitive detoxication are the most commonly reagents to eliminate lead in human body.[5] Unfortunately, other essential metal ions will also be eliminated at the same time. It is urgent to carry out the targeted drug release for lead; however, almost no existing methods could realize the goal. Here, we developed a biomimetic smart nano-device by modifying lead ( Ⅱ ) ions responsive DNAzymes onto the inner surface of ion-etched polymer nanochannels. Such a DNAzyme tunable lead (Ⅱ) ionic gate could be applied to fix-point drug release systems.

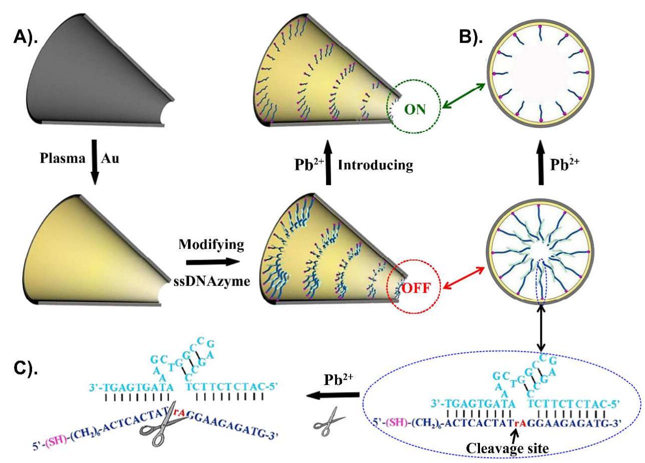


**Scheme 1** A). Preparation of lead (II) ions responsive gating; B). Mechanism of this ionic gating; C). The used ssDNAzyme and its $Pb^{2+}$-responsive mechanism.

Scheme 1 shows the fabrication process and the operating principle of the DNAzymes and nanochannel-based hybrid system (DNHS). Herein, the conical shaped nanochannel was prepared using an asymmetric track-etch technique with a poly ethylene terephthalate (PET, 12 µm thick) film, whose diameter at large opening side (base) was observed to be about 1.0 µm from the scanning electron microscopy (SEM) results (Fig. S1, ESI). The diameter at the narrow side (tip) was calculated to be around 40 nm using the reported method.[2h] Such a conical-shaped nanochannel can preferentially transport cations from the tip entrance to the base side of the channel if applied potential on both sides of the membrane, which is called rectification. Rectification emerges due to the channel asymmetry and electrostatic effects that are generated by the fixed charges created on the interior surface of the channel. The current rectification can be visualized by measuring current-voltage (*I-V*) curves under symmetrical electrolyte conditions (0.1 M KCl) (Fig. S2, ESI†).Once the conical nanochannel obtained, the gold will be sputtered into the inner surfaces of the channels from the base side for the modification of DNAzyme (Table 1) through Au-thiol bond. The reported "8-17" DNAzyme contains a chain (17-

DS) and an enzyme (17-E) component, which shows high activity and selectivity in the presence of $Pb^{2+}$.[6] The substrate (17-DS) is composed of a chain of DNA and RNA chimera, where an adenine nucleoside (rA) is at the cleavage site, and all of the residual bases are deoxyribonucleotides. In the presence of $Pb^{2+}$, the substrate chain is cleaved into two segments at the rA site, and the DNAzyme double-stranded portion becomes short single strands. After modification with DNAzyme, the "gate" shows "OFF" state at the very beginning because much longer DNAzymes block the ions transport. When $Pb^{2+}$ is introduced into this system, the "8-17" DNAzymes will be cleaved, and the "gate" shows "ON" state (Scheme 1) for the short 17-DS left lonely. The successful of DNAzyme grafting can be characterized by the XPS spectra (Fig. S3, ESI†). Clearly, the DNHS could exhibit excellent $Pb^{2+}$ recognition capability *via* the transformation from double-stranded portions to single residues.

**Table 1** Base sequences of the DNAzyme.

| *Name* | *Base Sequence* |
|---|---|
| 17-DS[a] | 5'-(SH)-$(CH_2)_6$-ACTCACTATrAGGAAGAGATG-3' |
| 17-E[b] | 5'-CATCTCTTCTCCGAGCCGGTCGAAATAGTGAGT-3' |
| 17-D[c] | 5'-(SH)-$(CH_2)_6$-ACTCACTATGGAAGAGATG-3' |

[a] DNAzyme 1, [b] DNAzyme 2, [c] DNAzyme 3.

Fig. 1A shows the *I-V* properties of the gold-sputtered nanochannels and after it was modified with ssDNAzymes (DNAzyme1+DNAzyme2) in the absence and presence of $Pb^{2+}$, respectively. We found that the gold-sputtered nanochannels rectified the ionic current, which might be ascribed to the negative charges coming from the adsorbed chloride anions (Square).[7] After ssDNAzymes were grafted onto the nanochannels, the ionic currents decreased remarkably because the electrolyte transporting across the channel driven by voltage was blocked by the stretched ssDNAzymes (Circle). When the DNHS exposed to $Pb^{2+}$, the current would increase remarkably (Triangle). The reason may stem from the enlarged ''effective pore size'' that was generated by the DNAzyme double-stranded portion cleaving into single strands (Scheme 1). Herein, the current ratios were calculated by the ionic currents that were measured in the presence of $Pb^{2+}$ *versus* the absence of $Pb^{2+}$ at 2 V. The $Pb^{2+}$ ion induced DNA strands changes could be characterized by the contact angle (Fig. S4, ESI†) measurement on the ssDNAzymes modified PET surfaces.

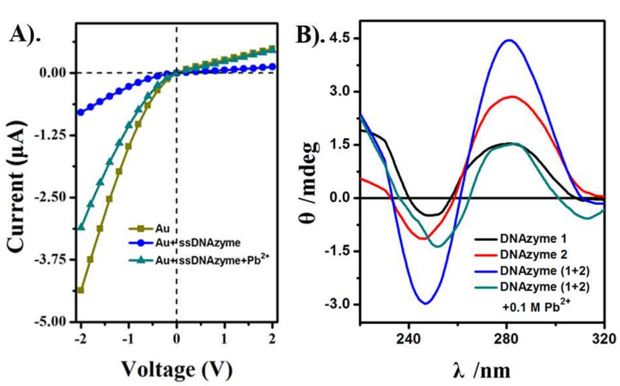


**Fig. 1** Current-voltage curves recorded in 0.1 M KCl on single conical nanochannels and the CD spectra. A) *I-V* curve that measured on the naked nanochannels after Au sputtered (Square), and *I-V* curves that measured on the nanochannels which grafted the ssDNAzyme before (Circle) and after (Triangle) $Pb^{2+}$ response; B) CD spectra of DNAzyme 1 (black), DNAzyme 2 (red), DNAzyme (1+2) (blue) and DNAzyme (1+2) in the presence of 0.1 M $Pb^{2+}$ (green).

The responsive property could be confirmed using CD spectroscopy, which is shown in Fig. 1B (ssDNAzymes) and Fig. 2A (nsDNAzymes (DNAzyme3+DNAzyme2)). DNAzyme1 and DNAzyme3 is the single-stranded responsive DNA and control DNA (no responsive), respectively. DNAzyme2 is a single-stranded DNA which can form double-strand with DNAzyme1 and DNAzyme3, which are ssDNAzymes (DNAzyme(1+2)) and nsDNAzymes (DNAzyme(3+2)). Before introducing lead ions, the CD spectra of ssDNAzymes and nsDNAzymes are basically the same, whether they are single or double stranded. After lead ions introduced, only ssDNAzymes can make the characteristic peak reduce. This is because the ssDNAzymes have a cleavage site (rA, in Scheme 1C) in the base sequence. This cleavage site which interacts with lead ion exhibits excellent capability *via* the double-stranded portion becoming single residue, which increases the effective pore size of the channels. Fig. 2B shows ion transportation of the gold-sputtered nanochannels, nsDNAzymes modified nanochannels, and nsDNAzymes modified nanochannels in the absence and presence of $Pb^{2+}$, respectively. The result showed the current of nsDNAzymes-grafted nanochannels (Circle) was similar to that of nsDNAzymes-grafted system even if the $Pb^{2+}$ was introduced (Triangle).

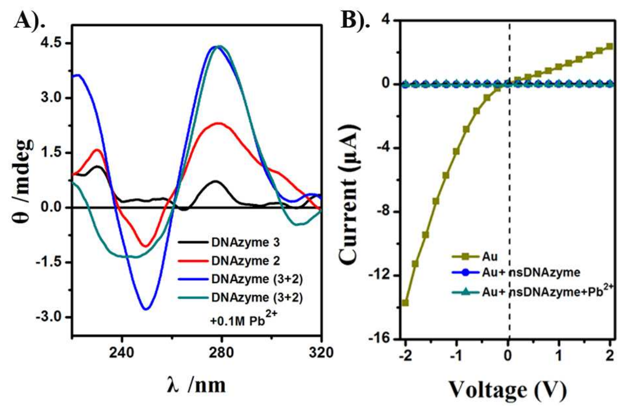


**Fig. 2** Current-voltage curves recorded in 0.1 M KCl on single conical nanochannels and the CD spectra. A) CD spectra of DNAzyme 3 (black), DNAzyme 2 (red), DNAzyme (3+2) (blue) and DNAzyme (3+2) in the presence of 0.1 M $Pb^{2+}$ (green). B) *I-V* curve that measured on the naked nanochannels after Au sputtered (Square), and *I-V* curves that measured on the nanochannels which grafted the nsDNAzyme before (Circle) and after introducing of $Pb^{2+}$ (Triangle).

The current-concentration (*I–C*) properties of the conical nano-channels are shown in Fig. S5. We selected five different $Pb^{2+}$ concentrations, 0.1 nM, 1 nM, 5 nM, 10 nM, 100 nM, respectively, for the responsive experiment. For the gold sputtered-nanochannels, the current decreased with increasing the concentration of $Pb^{2+}$. After grafting ssDNAzyme on the gold sputtered-nanochannels, the currents gradually increased with the concentration of lead (II) ranging from 0.1 to 5 nM. But the currents gradually decreased when the concentration of lead (II) increased from 5 to 100 nM. The largest current indicated that the ssDNAzymes showed the highest response, and the value was 5 nM. Thus, we chose this concentration as the optimal responsive concentration.

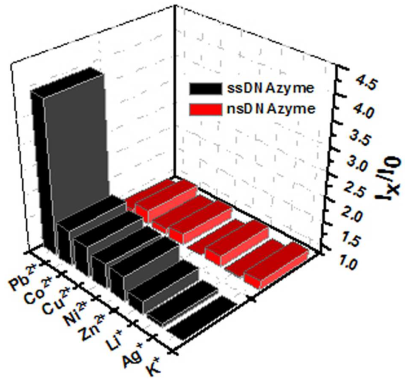


**Fig. 3** Current ratios measured at 1 V in ssDNAzyme and nsDNAzyme modified nanochannels interacting with different metal ions in 0.1 M KCl.

The selectivity of DNHS for $Pb^{2+}$ was evaluated by testing the response of the assay to other environmentally relevant metal ions, including $Co^{2+}$, $Cu^{2+}$, $Ni^{2+}$, $Zn^{2+}$, $Li^{+}$, $Ag^{+}$, and $K^{+}$ at a concentration of 5 nM. As shown in Fig. 4 (black column), the DNHS showed high selectivity towards $Pb^{2+}$, because there was a sharp increase in the current ratio when the DNHS was exposed to $Pb^{2+}$. This change could be attributed to the interaction between $Pb^{2+}$ ion and ssDNAzyme which had a cleavage site (rA) in the base sequence. The cleavage site interacted with lead ion and exhibited excellent capability *via* the double-stranded portion to a single residue, which increased the effective pore size of the nanochannels. Different from the ratio calculated by the ssDNAzyme modified nanochannels, the ratios calculated from nsDNAzyme modified nanochannels remained unchanged (red column), because the control nsDNAzyme could not interact with lead ions and thus the effect pore size and transport current remained constant.

## Conclusions

In summary, we developed a lead (II) gating based on ion-track etched PET membranes and $Pb^{2+}$ ion responsive DNAzyme. This smart nanodevice shows high sensitivity and selectivity to $Pb^{2+}$ but no other metal ions in the samples. Importantly, compared with protein based nanopores, this gate is robust which is stable in the changing external environments. Such an "abiotic" nanodevice constructed with a solidstate nanochannel and smart molecules provides a powerful platform for the targeting ion response and smart gating, which are important in the specific toxic ion removal. Therefore, we expect this innovative method could be applied to toxic ion ($Pb^{2+}$) recognition and target drug release, and achieve the ideal effects on lead eliminating.

We thank the Material Science Group of Institute of Modern Physics, Chinese Academy of Sciences for providing the ion-irradiated samples. This work was supported by the National Research Fund for Fundamental Key Projects (2011CB935703), National Natural Science Foundation (21171171, 21434003, 21201170, 21473213, 91127025, 91427303, 21421061, 61001051), and the Key Research Program of the Chinese Academy of Sciences (KJZD-EW-M01, KJZD-EW-M03).

## Notes and references

[a] *College of Chemistry and Environmental Science, Key Laboratory of Analytical Science and Technology of Hebei Province,, Hebei University, Baoding, Hebei Province, 071002, P. R. China*
[b] *Laboratory of Bio-inspired Smart Interfacial Science, Technical Institute of Physics and Chemistry, Chinese Academy of Sciences, Beijing 100190, P. R. China. E-mail: wlp@iccas.ac.cn;*
*Tel: +86-10-82621396*
[c] *College of Chemistry and Chemical Engineering, Yan'an University, Yan'an, Shaanxi Province, 716000,*
[d] *Beijing National Laboratory for Molecular Sciences (BNLMS), Key Laboratory of Organic Solids, Institute of Chemistry, Chinese Academy of Sciences, Beijing 100190, P. R. China.*

† Electronic Supplementary Information (ESI) available: [details of any supplementary information available should be included here]. See DOI: 10.1039/b000000x/

Y. S., Y. Z., and P. L. are equally to this work.

1. (a) B. Eisenberg, *Acc. Chem. Res.* 1998, **31**, 117; (b) E. Perozo, D. M. Cortes, P. Sompornpisut, A. Kloda, B. Martinac, *Nature* 2002, **418**, 942; (c) O. Beckstein, P. C. Biggin, P. Bond, J. N. Bright, C. Domene, A. Grottesi, J. Holyoake, M. S. P. Sansom, *Febs Lett.* 2003, **555**, 85; (d) M. Ali, S. Nasir, I. Ahmed, L. Fruk, W. Ensinger, *Chem. Commun.* 2013, **49**, 8770.
2. (a) Z. S. Siwy, *Adv. Funct. Mater.*, 2006, **16**, 735; (b) X. Hou, W. Guo, F. Xia, F.Q. Nie, H. Dong, Y. Tian, L. Wen, L. Wang, L. Cao, Y. Yang, J. Xue, Y. Song, Y. Wang, D. Liu and L. Jiang, *J. Am. Chem. Soc.*, 2009, **131**, 7800; (c) Y. Tian, X. Hou, L. Wen, W. Guo, Y. Song, H. Sun, Y. Wang, L. Jiang and D. Zhu, *Chem. Commun.*, 2010, **46**, 1682; (d) L. Wen, X. Hou, Y. Tian, F.Q. Nie, Y. Song, J. Zhai and L. Jiang, *Adv. Mater.*, 2010, **22**, 1021; (e) Y. Tian, Z. Zhang, L. Wen, J. Ma, Y. Zhang, W. Liu, J. Zhai and L. Jiang, *Chem. Commun.*, 2013, **49**, 10679; (f) L. Lin, J. Yan, and J. Li, *Anal. Chem.*, 2014, **86**, 10546; (g) J. Lee, M. Kim, S. Jin, H. Lee, Y. K. Kwon, H. J. Park and C. Kim, *New J. Chem.*, 2014, **38**,4652; (h) L. Gao, P. Li, Y. Zhang, K. Xiao, J. Ma, G. Xie, G. Hou, Z. Zhang, L. Wen and L. Jiang, *Small*, 2015, **11**, 543.
3. Z. S. Siwy, M. R. Powell, A. Petrov, E. Kalman, C. Trautmann and R. S. Eisenberg, *Nano Lett.*, 2006, **6**, 1729.
4. C. Zhao, X. Li, L. Li, X. Gong, Y. Chang and J. Zheng, *Chem. Commun.*, 2013, **49**, 9317.
5. (a) J. Osterloh and C. E. Becker, *Clin. Pharmacol. Ther.*, 1986, **40**, 686; (b) N. P. Goldraich, O. L. Ramos and I. H. Goldraich, *Pediatr. Nephrol.*, 1989, **3**, 1; (c) J. F. Rosen, M. E. Markowitz, P. E. Bijur, S. T. Jenks, L. Wielopolski, J. A. Kalefezra and D. N. Slatkin, *Proc. Natl. Acad. Sci. USA*, 1989, **86**, 685; (d) E. Bjorgvinsson, M. Majd and K. D. Eggli, *Am. J. Roentgenol.*, 1991, **157**, 539; (e) J. F. Rosen, M. E. Markowitz, P. E. Bijur, S. T. Jenks, L. Wielopolski, J. A. Kalefezra and D. N. Slatkin, *Environ. Health. Persp.*, 1991, **93**, 271.
6. P. Y. Apel, Y. E. Korchev, Z. Siwy, R. Spohr and M. Yoshida, *Nulear.Instru.Math.Phys.Res.B*, 2001, **184**, 337.
7. J. Liu, Y. Lu, *Anal. Chem.*, 2003, **75**, 6666.
8. (a) S. Biggs, P. Mulvaney, C. F. Zukoski and F. Grieser, *J. Am. Chem. Soc.*, 1994, **116**, 9150; (b)L. T. Sexton, L. P. Horne and C. R. Martin, *Mol. Biosyst.*, 2007, **3**, 667.